

Microstructures of a phosphatic crust from the Peruvian continental margin: phosphatized bacteria and associated phenomena

Phosphogenesis
Phosphorites
Microbial mediation
Sedimentary petrology
Peruvian margin
Phosphatogenèse
Phosphates
Actions microbiennes
Petrologie sédimentaire
Marge péruvienne

Michel LAMBOY

Département de Géologie, Université de Rouen, B.P. 118, 76134 Mont-Saint-Aignan Cédex, France.

Received 10/07/89 in revised form 14/12/89, accepted 20/3/90.

ABSTRACT

Detailed petrographic observations, by scanning electron microscopy, have been conducted on a Recent, oriented phosphatic crust from the Peruvian continental margin, which has been the subject of several physico-chemical studies. Within the crust, apatite appears as ovoid particles, interpreted by some authors as inorganic precipitates. These particles are associated with minute filaments. They are flattened against detrital minerals and tests, irregularly inserted in more or less precise mouldings of partially or totally dissolved diatom frustules. It is suggested here that these micron-sized particles correspond to phosphatized bacteria. In the lower part of the crust, which is also the oldest part, overgrowth and/or recrystallization have transformed ovoidal particles into elongated hexagonal apatite crystals. The invasion of the sediment by bacteria, their mineralization, and the dissolution of associated opal, are discussed. Similar histories of bacterial moulding and substrate dissolution have been suggested for phosphorites from Tunisia and northern France.

Oceanologica Acta, 1990, 13, 4, 439-451.

RÉSUMÉ

Microstructures d'une croûte phosphatée de la marge continentale du Pérou: bactéries phosphatisées et phénomènes associés

Des observations pétrographiques détaillées en microscopie électronique à balayage ont été réalisées sur une croûte phosphatée récente de la marge continentale du Pérou, d'orientation connue, et ayant fait par ailleurs l'objet de plusieurs études physico-chimiques. L'apatite se présente en globules ovoïdes, qui résulteraient, selon certains auteurs, d'une précipitation inorganique. Ces globules, associés à de fins filaments, aplatis et déformés au contact des particules détritiques, irrégulièrement engagés dans des moulages plus ou moins précis de frustules de diatomées partiellement ou totalement dissous, correspondraient à des bactéries phosphatisées. Dans la partie inférieure de la croûte, la plus ancienne, une surcroissance cristalline et/ou une recrystallisation ont transformé les globules ovoïdes en cristaux hexagonaux allongés d'apatite. L'invasion du sédiment par les bactéries, leur minéralisation, et les dissolutions associées sont discutées. Les informations apportées par cette étude sont cohérentes avec celles provenant d'autres études effectuées sur des phosphorites de Tunisie et du Nord de la France par des méthodes semblables.

Oceanologica Acta, 1990, 13, 4, 439-451.

INTRODUCTION

Phosphorites from the seafloor and from the ore deposits on continents are composed of grains, crusts, and nodules. The petrography of the phosphatic sediments and rocks from both sources is very complex and numerous proposals exist for the genesis of apatite

mineral and the phosphatic particles (Slansky, 1980, 1986).

Phosphatized microbial remains have been described in present day sea-bed phosphorites (O'Brien *et al.*, 1981; Purnachandra Rao and Nair, 1988) and from numerous ancient economic phosphate deposits on land (Soudry and Champetier, 1983; Zanin *et al.*, 1985,

1987; Southgate, 1986; Soudry, 1987; Lamboy and Monty, 1987, 1990; Soudry and Lewy, 1988; Lamboy, 1987*b*, 1989; Soudry and Southgate, 1989). Synthesis of apatite by bacterial activity has been realized in the laboratory (Lucas and Prévôt, 1981, 1985, 1988).

The sediments on the continental margin off Peru contain phosphatic crusts, nodules, and grains; they have been the subject of numerous studies, especially physico-chemical ones (for references, see the special issue of *Marine Geology*, 1988, 80, 3-4). They constitute one of the few settings where recent phosphatization has been described (Veeh *et al.*, 1973; Burnett *et al.*, 1980); along with the Mexican margin (Jahnke *et al.*, 1983), the African margin off Namibia (Baturin, 1982), and the Australian margin (O'Brien and Veeh, 1980).

This paper reports detailed scanning electron microscopy (SEM) observations on an oriented phosphatic crust from the Peruvian continental margin. The objective was to enlarge our understanding of the mechanisms of apatite formation and the possible role of microbes in the crust's genesis, and to compare these observations with similar studies of other phosphorites of different localities and age.

MATERIAL AND METHODS

Sample GS 1N (studied here) is a piece of phosphatic crust recovered during cruise 23-06 of the R/V *Robert D. Conrad* off the coast of Peru in June-July 1982, from 7°36.3'S and 80°38.0'W at a water depth of 480 m (Burnett and Froelich, 1988). Obtained with a grab corer, the crust was covered by 14 cm of sediment; thus, its orientation with respect to top vs. bottom is known (Kim and Burnett, 1986). Several recent studies have been made on other pieces of this crust: determination of sedimentation rate and growth direction using

uranium-series radionuclides (Kim and Burnett, 1986), rare earth elements composition (Piper *et al.*, 1988), carbon-isotopic composition and lattice-bound carbonate concentrations (Glenn *et al.*, 1988), and petrology (Glenn and Arthur, 1988). Other studies concern the crust-associated sediment (Kim and Burnett, 1988; Glenn and Arthur, 1988), or nodules and phosphatic grains (Kim and Burnett, 1985; Cunningham and Burnett, 1985; Burnett and Kim, 1986; Glenn and Arthur, 1988), and the prevailing sediments (Froelich *et al.*, 1988) in the same area.

The sample was dried at room temperature and sawn perpendicularly to its top surface. A thin section and a polished surface were examined with binocular and optical microscopes. Numerous representative small fragments were broken from the crust and their positions were precisely recorded; some were ultrasonically treated to remove dust, immediately coated with gold-palladium without acid etching, before examination under SEM (Jeol T20). Point analyses were made (energy spectra obtained by a ORTEC system coupled to a SEM Jeol 35CF). Additional observations by transmission electron microscopy (TEM) were also conducted (Philips EM 300).

RESULTS AND DISCUSSION

General presentation of the sample

The dried sample has a dull earthy surface and its colour is light brownish-gray; a dark, non-phosphatic mud adheres to its surface here and there. Several cylindrical holes cross the crust fragment (Fig. 1). They are due to boring organisms, obviously active after phosphatization because the walls clearly cut the crust and because the mud covering these walls is not phosphatic. The crust section shows traces of intense bio-



Figure 1

Oriented sawn cross-section of the studied fragment of phosphatic crust. The infillings of the numerous burrows (while arrows), which are underlined by small curved laminae, are phosphatized. A large open boring crosses the crust. In the upper part, the vertical sawmarks indicate the hardest parts of the crust. The scattered small black grains are glauconite grains. For a, b, c, see text.

Section sciée et orientée du fragment de croûte étudié. Les remplissages des nombreux terriers (flèches blanches), soulignés par de fines lamines courbes, sont affectés par la phosphatisation. Une grosse perforation traverse la croûte. Les petites taches noires dispersées sont des grains de glauconie. En a, mince niveau supérieur, clair, friable, le plus jeune (4790 ans d'après Kim et Burnett, 1986); en b, niveau moyen plus sombre et plus consolidé, irrégulier, souligné par des traces de sciage; en c, partie basale, claire et friable.

turbation as noted by Piper *et al.* (1988, p. 271). The burrow infillings are phosphatized (Fig. 1). Numerous glauconite grains of light green or dark green colour are scattered throughout the crust.

The crust is vertically divided into 3 zones. A poorly lithified, light-coloured layer, about 2 mm thick ("a" on Fig. 1), covering the top surface, corresponds to the youngest part of the crust (4790 years according to Kim and Burnett, 1986). Under this topmost layer, the major part of the upper half of the crust has a darker colour and a shiny aspect on polished slab. On Figure 1, sawmarks indicate the location of this harder area ("b") whose lower limit is irregular. The light-coloured lower half has poor cohesion ("c" on Fig. 1); its base corresponds to the oldest part of the crust (6500 years according to Kim and Burnett, 1986). This description is similar to those of other pieces of the crust (Kim and Burnett, 1986; Piper *et al.*, 1988) and of one homogeneous phosphatic nodule recovered at the same location (Glenn and Arthur, 1988, Fig. 3 A). Thin section observations on the studied fragment are similar to those published by Piper *et al.* (1988, Fig. 2 F). The fine-grained apatite matrix appears homogeneous and pseudoisotropic; it corresponds to the interstitial phosphatic cements described by Glenn and Arthur (1988).

Under SEM, at low magnification, observation of small fragments from various locations in the crust reveals rounded, cracked glauconite grains, numerous diatom frustules of several species, detrital particles made up essentially of quartz and feldspar as deduced by microprobe analysis, and imprints which often correspond to diatoms (Fig. 2). Except for the largest frustules of centric diatoms, diatom remains cannot be recognized under the binocular lens. The observation of apatite particles and, hence, a petrographic analysis of the mechanisms of phosphate genesis (or processes related to this genesis), requires high magnifications.

The apatite particles

Apatite essentially appears in small "rod-shaped" particles more or less ovoidal, 0.8 to 1.5 μm in length and 0.3 to 0.5 μm in width (Figs. 3 to 9). Apatite particles are isolated or in groups of two, three, or more, forming rosettes and agglomerates. They are comparable to those described earlier in Peruvian phosphatic nodules (Burnett, 1977; Burnett *et al.*, 1980; Glenn and Arthur, 1988). Point microprobe analyses have been made on agglomerates of apatite particles. The results are in agreement with those already made on Peru phosphorites by similar methods (Burnett, 1977; Glenn and Arthur, 1988; Piper *et al.*, 1988). Some minute filaments and some ovoidal or subspherical particles, 0.1 to 0.5 μm in diameter, are present in addition to the rod-shaped ones; because of their very small size, their apatitic composition is often difficult to prove by microprobe analysis.

Rod-shaped apatite particles with similar sizes and shapes have been observed in numerous phosphorites on the seafloor and on continents. Most authors attribute a diagenetic origin to these particles. However, a fundamental divergence exists in the interpretation of the mechanism by which these particles form. Schematically, for some authors they develop by inorganic crystallization (Burnett, 1977; Bremner, 1980; Baturin, 1982; Mullins and Rasch, 1985; Glenn and Arthur, 1988; Reimers *et al.*, 1989) while for others they correspond to phosphatized bacteria (O'Brien *et al.*, 1981; O'Brien and Veeh, 1983; Soudry, 1987; Zanin *et al.*, 1987; Lamboy and Monty, 1987, 1990; Soudry and Lewy, 1988; Purnachandra Rao and Nair, 1988; Fikri *et al.*, 1989; Lamboy, 1989; Br  h  ret, 1990). Inorganic precipitation can certainly lead to crystals whose size and shape suggest bacterial or microbial colonies (*see*, for example, Bayer and Wiedemann, 1989). However, an analysis of the structures of the Peruvian

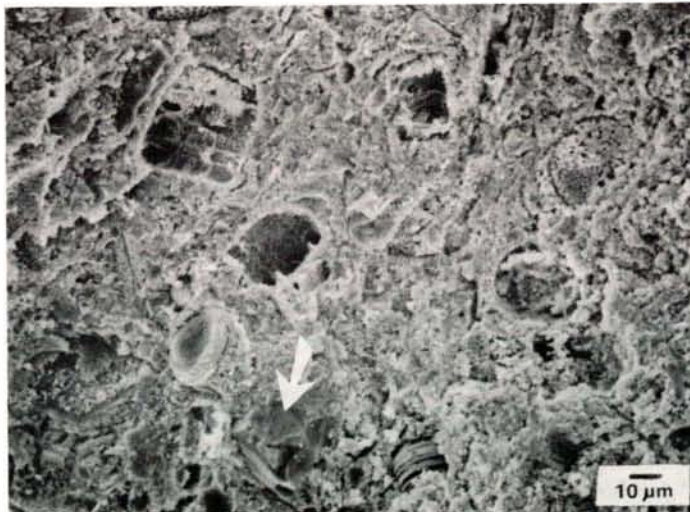


Figure 2

Representative view of the phosphatic crust as seen under scanning electron microscope at low magnification. Some frustules of different types of diatoms and imprints of diatom frustules can be observed. Small detrital particles (quartz and feldspar according to microprobe analysis) are common (arrow). Between frustules and detrital particles, the phosphatic matrix appears.

Aspect repr  sentatif de la cro  te phosphat  e au microscope   lectronique    balayage et    faible grandissement. Des frustules de diatom  es de diff  rents types avoisinent des empreintes attribuables    d'autres frustules. De fines particules d  tritiques (quartz et feldspaths d'apr  s microsonde) sont souvent visibles (fl  che). Entre ces   l  ments, apparait la matrice phosphat  e.

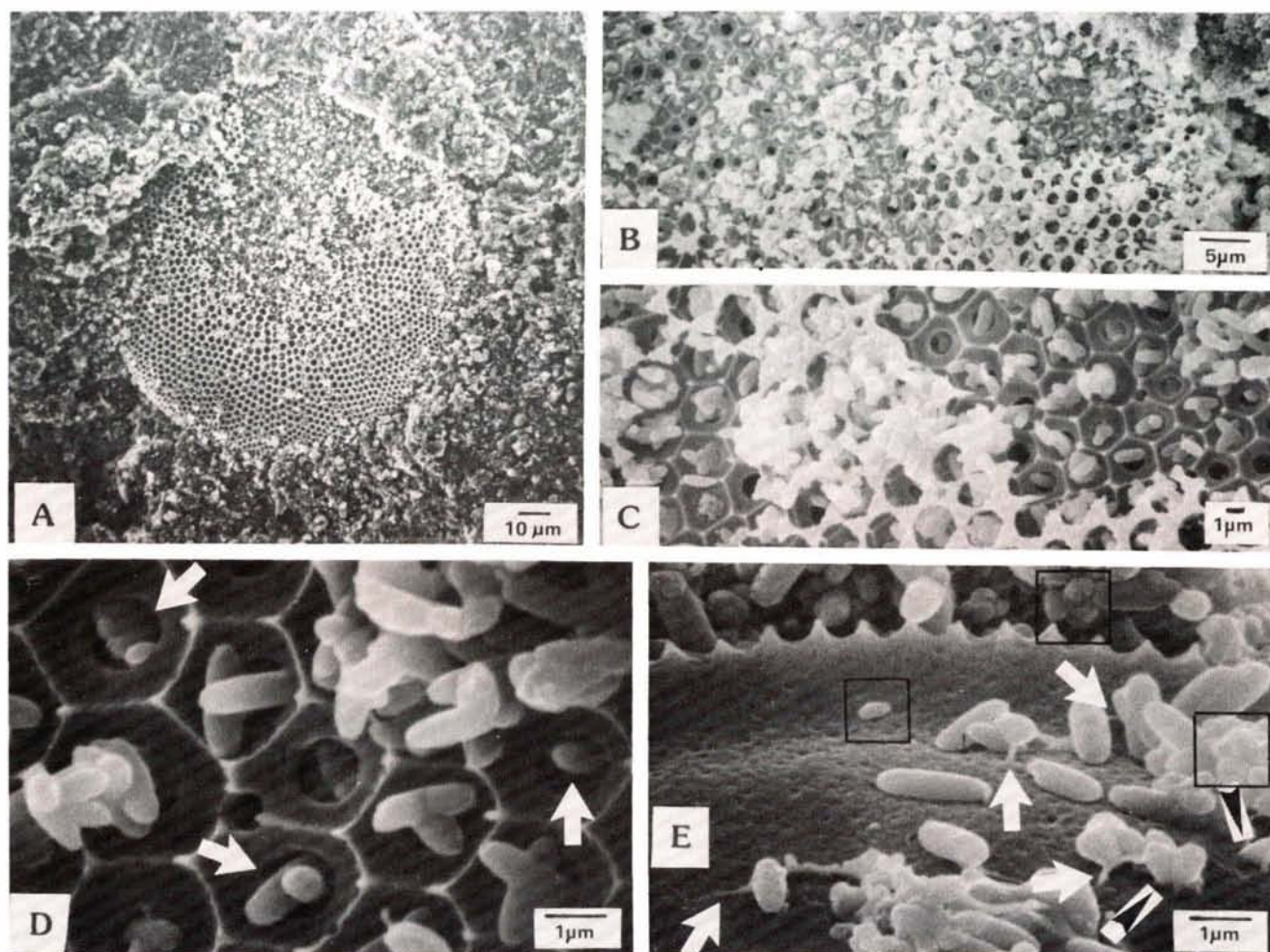


Figure 3

Rod-shaped apatite particles in the neighbourhood of a diatom frustule. A: large diatom frustule included in the phosphatic matrix. B and C: enlarged segments of A. The frustule valve shows a double wall: the dark and continuous inner wall is pierced by small pores; the outer one, light-coloured and sometimes absent, has large pores. D: detail of C. The structure of the frustule's inner wall is clearly visible. The elongated ovoidal masses, 1 to 2 µm length, isolated or agglomerated in various ways, are the principal form of phosphate particles; they are not stuck to the test's silica and many of them emerge through the pores (arrows). E: ovoidal phosphatic masses close to a rather smooth valve of another kind of diatom. Thin filaments (white arrows) coming from one ovoidal mass link up another mass or the frustule surface (in this case, they appear to penetrate micropores of the wall). Some ovoidal apatite particles are flattened against the frustule (black arrows). All the elongated phosphatic masses are interpreted as phosphatized bacterial bodies. Other small phosphatic corpuscles, subspherical or ovoidal, 0.3 to 0.5 µm in length, isolated or agglomerated (squares in 3 E), may represent other bacterial species or bacteria partly fossilized by phosphate.

Bâtonnets d'apatite au voisinage d'un frustule de diatomée. A: grand frustule inclus dans la matrice phosphatée. B et C: détails successifs de A. La valve du frustule montre une double paroi: la paroi interne, continue et sombre, est percée de petits pores; la paroi externe, claire, absente par endroits, possède des pores de grande taille. D: détail de C. La structure de la paroi interne du frustule est bien visible. Les masses ovoïdes allongées, longues de 1 à 2 µm, isolées ou diversement agglomérées, correspondent à l'aspect dominant des particules de phosphate; elles ne sont pas adhérentes à la silice du test et beaucoup sortent des pores (flèches). E: masses ovoïdes phosphatées contre une valve assez lisse d'un autre type de diatomée. De fins filaments (flèches blanches) issus de ces masses ovoïdes les relient à d'autres masses ou à la surface du frustule (ils semblent alors pénétrer dans les microporations de la paroi). Quelques particules ovoïdes sont aplaties contre le frustule (flèches noires). Toutes ces masses ovoïdes allongées sont interprétées comme des corps bactériens phosphatisés. D'autres petits globules phosphatés, subsphériques ou ovoïdes, de 0,3 à 0,5 µm, isolés ou agglomérés (carrés noirs sur 3 E), pourraient être d'autres formes bactériennes ou des bactéries partiellement fossilisées par le phosphate.

crust yields features which lead the present author to consider the rod-shaped apatite particles as phosphatized bacteria.

The phosphatic matrix between the diatom remains and the detrital particles (Fig. 2), making up the bulk of the crust, is constituted by agglomerates (Fig. 4), the study of which provides scant information. In these agglomerates, rod-shaped particles prevail, with a generally regular morphology. They are somewhat densely packed, and it is difficult to distinguish filaments, smaller ovoidal particles, or small non-phosphatic fragments. The rod-shaped apatite particles are not uniformly oriented and it is impossible to prove that one of them was a nucleation substrate for another.

Porosity of Peru sediments where phosphatization appears is very high ($>0,96 \text{ ml cm}^{-3}$, Froelich *et al.*, 1988). Therefore, in the crust, the areas of phosphatic matrix probably correspond to phosphatization of large pores of the initial sediment. Petrologic study of Peru margin phosphorites (Glenn and Arthur, 1988) shows that apatite displays a preference for nucleation on preexisting hard substrates and frequently an oriented growth. The SEM investigations of the phosphatic matrix presented here do not show regular texture or polarity corresponding to an oriented chemical growth. SEM investigations in the neighbourhood of non-phosphatic particles bring more interesting information.

At moderate magnification, the general size and shape

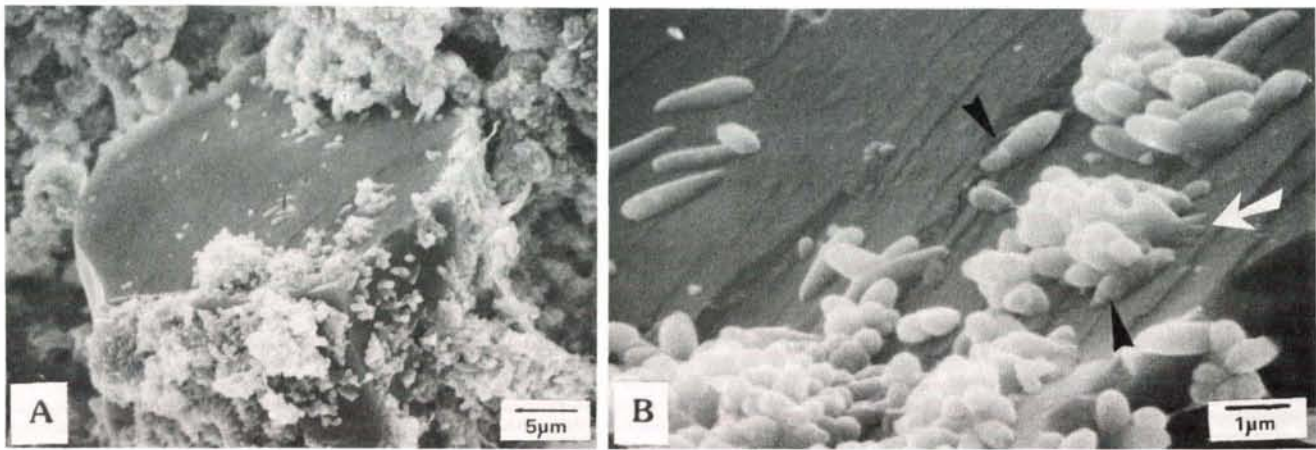


Figure 4

Deformation of rod-shaped apatite particles close to detrital particles. A: representative appearance of a quartz grain inside the agglomerates of rod-shaped particles constituting the phosphatic matrix. B: detail of A. Irrespective of the orientation of their long axis on the quartz surface, numerous apatite particles are flattened against this surface; some of them have a "fixation foot" (white arrow). Note filaments and ovoidal morphologies with constrictions (black arrows).

Déformation des bâtonnets d'apatite contre des particules détritiques. A: aspect représentatif d'un quartz au sein des agglomérats de bâtonnets constituant la matrice phosphatée. B: détail de A. Quelle que soit l'orientation de leur grand axe par rapport à la surface du grain de quartz, beaucoup de bâtonnets sont aplatis contre cette surface; certains développent un « pied » de fixation (flèche blanche). Noter aussi, outre des filaments, des bâtonnets présentant des constrictions (flèches noires).

of the rod-shaped particles seem similar from the bottom to the top of the crust. A morphological difference, however, can be observed at very high magnification between particles from the upper and the lower parts. In the topmost layer and in the upper, indurated half, apatite particles show subcircular sections and rounded ends (Figs. 3 D, 3 E, 6 B). Their morphology is similar to those of "phosphatized bacteria" reported in phosphorites from the Australian margin (O'Brien *et al.*, 1981) and the Indian margin (Purnachandra Rao and Nair, 1988). They also closely resemble the bacteria experimentally phosphatized by Lucas and Prévôt (1981, 1985, 1988) and El Faleh (1988). Most of the rod-shaped apatite particles located in the pulverulent

bottom part consist of elongated, more or less regular hexagonal crystals (Figs. 5 A, 9 B) clearly recognizable under TEM (Fig. 5 B). The spatial separation of ovoid and prismatic apatite particles is probably more complex than the one schematized here. The term "rod-shaped particles" will be used here in a general sense, embracing both prismatic and ovoid types.

We never observe a break in a rod-shaped particle; their internal cohesion is much stronger than that between either the apatite particles or between apatite and other particles. Under TEM, the apatite particles have a solid appearance (Fig. 5 B). In the neighbourhood of diatom frustules and detrital quartz and feldspar grains, the rod-shaped apatite particles may have

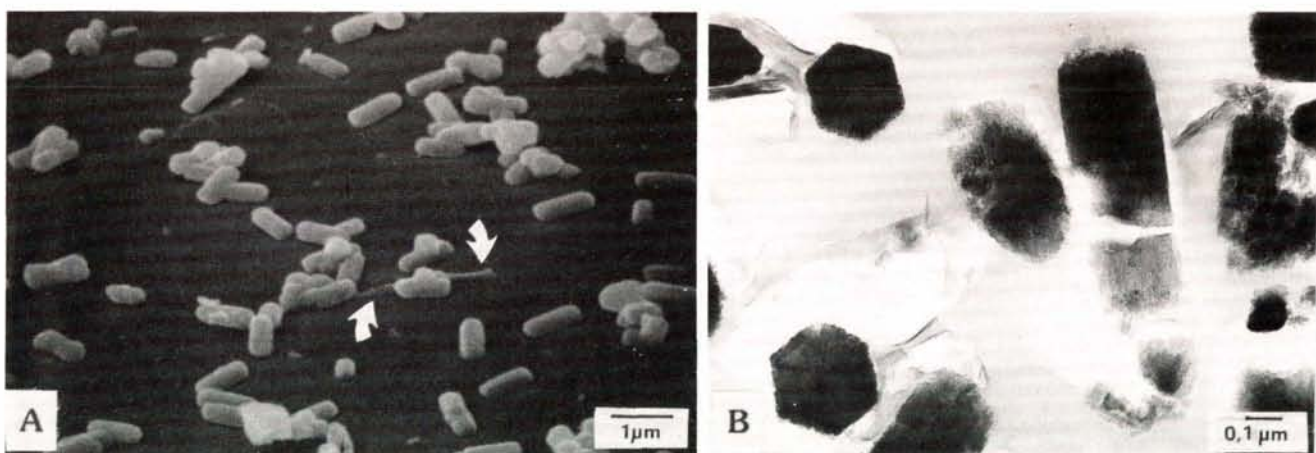


Figure 5

Some aspects of apatite particles in the lower pulverulent part of the crust. At A, on a quartz surface, the few sharpened rod-like apatite particles appear to have an hexagonal section; some of them are flattened against the quartz, and some filaments (white arrows) are associated with them (diatom moulding also exists as proved by figure 9 B which also shows this pulverulent part). At B, transmission electron microscopy clearly shows morphology of hexagonal prisms; however, at the centre, an oval oblique section corresponds to an ovoidal rod-like particle. Each hexagonal prism is thought to correspond to a bacterial body whose morphology was modified by apatitic overgrowths and/or recrystallization.

Aspect des particules d'apatite dans la partie inférieure pulvérulente de la croûte. En A, à la surface d'un quartz, les bâtonnets d'apatite peu effilés à leurs extrémités semblent avoir une section hexagonale; certains sont aplatis contre le quartz et quelques filaments (flèches) leur sont associés (le moulage des tests de diatomées est également réalisé comme le montre la figure 9 B prise dans cette partie pulvérulente). En B, la microscopie à transmission révèle clairement la morphologie en prisme hexagonal; toutefois, au centre du cliché, une section oblique ovale traduit un bâtonnet ovoïde. Chaque prisme hexagonal correspondrait à un corps bactérien modifié dans sa morphologie par des surcroissances apatitiques et/ou une recrystallisation.

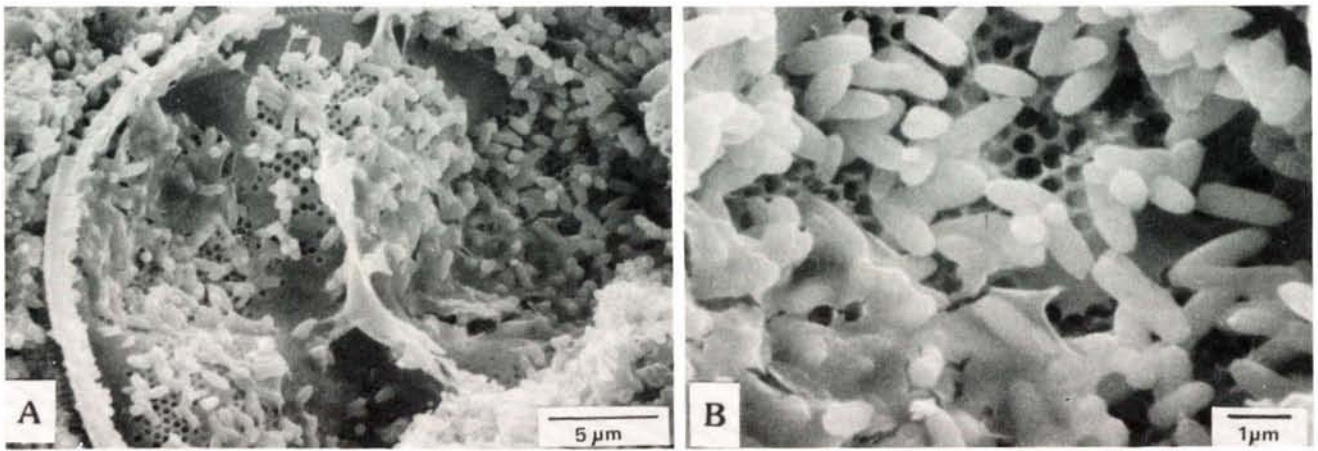


Figure 6

Rod-shaped apatite particles associated with organic matter in a diatom frustule. This organic matter was dark-coloured under binocular lense. A: general aspect of the veil of organic matter, pleated in the central part and partially covering the pores of the frustule. B: detail of A in the centre of the right half. In the lower left quarter, "phosphatized bacteria" and associated smaller apatitic particles are inside the cracked thin veil of organic matter.

Bâtonnets d'apatite au sein de matière organique contenue dans un frustule de diatomée. Cette matière organique apparaissait en sombre à la loupe binoculaire. En A, aspect général du voile de matière organique, plissé dans sa partie centrale, et recouvrant partiellement les pores du frustule. En B (détail de A dans la partie droite et vers le milieu), les «bactéries» et les petites particules apatitiques associées sont dans le fin voile craquelé de matière organique.

a regular or irregular morphology. The regular ones are not stuck to frustules and grains and in these cases it does not appear that substrate acts as a nucleation site for apatite. Instead they appear to develop in cavities, such as the inside of diatom valves (Figs. 3, 6, 9) or the areoles of the bilamellar-structured frustules (Figs. 3, 9), agglomerating themselves in a non-systematic manner. When organic matter is present (Fig. 6), apatite particles are intimately associated with it. The irregular rod-shaped apatite particles very often show a flattening against the support (Figs. 3 E, 4 B, 5 A, 8 B, 8 C, 9 B) and sometimes constrictions (Fig. 4 B) or a deformation which looks like a "fixation foot" (Fig. 4 B). The orientation of flattening is not related to the long axis of the apatite particles. Such non-systematic deformations do not appear to be linked to apatite nucleation or crystalline growth.

Although it cannot be ruled out, direct inorganic apatite nucleation on mineral substrates as proposed by Burnett (1977) and numerous other authors does not appear to be an evident mechanism of the production of the observed structures. However, inorganic precipitation of apatite may produce ovoidal/spherical particles of nearly constant size which flatten on solid substrate (Van Cappellen, pers. comm.). All these structures, and others that will be discussed below, evoke bacteria that colonized in an irregular fashion in inter- and intra-granular pore spaces, more or less filled with organic matter. These bacteria seem to have agglomerated and flattened against obstacles, without any particular orientation. Moreover, phosphatic filaments emerge from rod-shaped apatite particles (Figs. 3 D, 3 E, 4 B, 5 A, 6 B) and link up one phosphatic particle to another, and/or to the surfaces of frustules and quartz and feldspar grains. They may correspond to the remains of outer-coat bacterial mucous expansions, or of the glycocalix which permits bacteria to adhere to a substrate (Costerton *et al.*, 1978). Such mineralized filaments have been observed in various phosphorites

and interpreted in this way, whether they are associated only with phosphatized bacteria (Zanin *et al.*, 1985) or also with phosphatized microbial colonies (Lamboy and Monty, 1987, 1990).

Mechanisms of apatite fixation are not clearly established in the experiments on bacterial precipitation of apatite. Because of the preservation of bacteria morphology, a nucleation on the bacterial membrane is probable (El Faleh, 1988), but an extracellular precipitation has also been suggested for tiny apatite particles (Vaillant, 1987). The necessary presence of bacteria to obtain precipitation in experiments incites us to believe that initial nucleation of nanocrystals of apatite, or of a non-apatitic precursor (Van Cappellen and Berner, 1989), occurs *in vivo*. Because the phosphatized bacterial bodies observed in experiments and in natural phosphorites are not hollow, other nanocrystallites are necessarily joined *post mortem*. The prismatic habit of apatite particles in the bottom part of the crust may be a morphological signature of overgrowth or recrystallization. Thus, the lower part of the crust may be more evolved (*i.e.* may have been submitted to phosphogenesis during a longer period). This is in agreement with measured crust ages, which show a crust growth in the sediment from the bottom towards the top, and to crystallographical analysis showing a better crystallinity of apatite in the lower part of the crust (Kim and Burnett, 1986). In other phosphorites, further crystal growth leads to the local appearance of smooth crystalline faces on ovoid bacteria-like apatite particles (Lamboy and Monty, 1987, 1990) and on microbially mediated globose structures (Soudry and Lewy, 1988).

Neither the well-crystallized, flat hexagonal apatite crystals observed in some submarine phosphatic nodules (O'Brien *et al.*, 1981; Cullen and Burnett, 1986; Purnachandra Rao and Burnett, 1989), nor the well-crystallized squat crystals, several micrometres in

length, observed in phosphorites from the south-west African margin (Baturin and Dubinchuk, 1979) are found in the crust studied. It also seems that this crust does not contain the mineralized sheaths interpreted as cyanobacterial remains and observed in numerous phosphorites (Soudry and Champetier, 1983; Southgate, 1986; Soudry, 1987; Garrison *et al.*, 1989), or phosphatized microbial colonies (Lamboy and Monty, 1987, 1990; Soudry and Lewy, 1988; Lamboy, 1989). The ovoidal and prismatic rod-shaped particles which constitute the bulk of apatite in the crust may be phosphatized bacteria. The crust may contain concentrations of the order of several hundred billion of these fossilized bacteria per cubic centimetre. The smaller apatite particles may correspond to other bacterial species, and/or to incompletely mineralized bacteria, and/or to bacterial extracellular precipitates, and/or other phenomena.

Most of phosphatic sediments of the Peruvian margin are covered by a thick microbial mat composed largely of *Thioplaca* sp. Froelich *et al.* (1988) consider that the (inorganic) precipitation of apatite is linked to the early diagenesis of organic matter in the upper few centimetres of the sediment. Phosphate concentrations in interstitial waters may be controlled by the metabolism of the *Thioplaca* mat, as also suspected by other authors (Reimers, 1982; Williams and Reimers, 1983; Reimers *et al.*, 1989; Garrison *et al.*, 1989), although

other alternatives have been suggested for the phosphorus supply (Froelich *et al.*, 1988; Glenn and Arthur, 1988; Glenn *et al.*, 1989). The crust studied here does not contain significant traces of cellular chains or mucilaginous veils from filamentous bacteria which may correspond to the remains of *Thioplaca* mats. Therefore, the phosphatized bacteria in the crust seem to belong to other bacterial communities which remain to be identified. However, the production of dissolved phosphate could take place predominantly inside the *Thioplaca* mat (this mat may constitute a nutrient supply for other bacterial communities) and diffusion could transport the dissolved phosphate downward, towards the precipitation area (Van Cappellen and Berner, 1988).

Dissolution of opal of diatom frustules

High dissolved pore-water silica have been measured in interstitial water of the sediments from the Peruvian margin (Froelich *et al.*, 1988) which proves that opal dissolution take place in these sediments. In the phosphatic crust, the diatom frustules are frequently incomplete. Sometimes, they have clearly been broken during sample preparation (Figs. 8 A to 8 C). In other cases, part of a frustule is absent (Figs. 3 A to 3 C, 7 C, 9 A, 9 D) and it is difficult to distinguish between break and dissolution. But, partial (Figs. 7 B, 9 C) or total

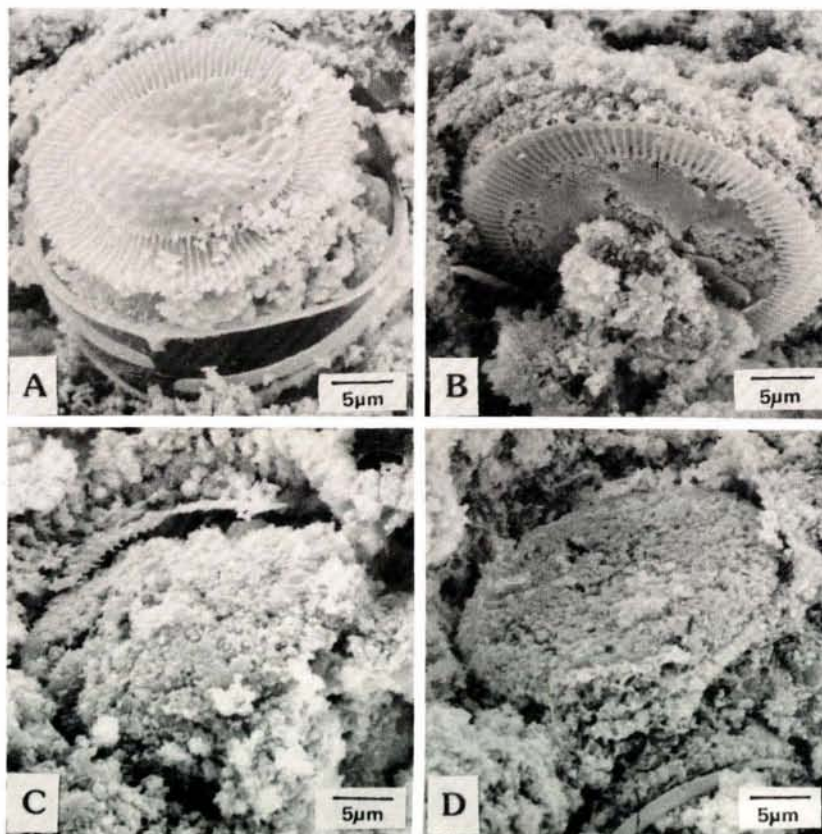


Figure 7

Dissolution of monolamellar frustule valves associated with a crude phosphatic mould. A: non-dissolved frustule; note the abundance of rod-shaped apatite particles between the disconnected valves. Frustule dissolution is incipient in B, partial in C, and complete in D. In the absence of a non-dissolved frustule fragment, only the general morphology of the very porous structure permits recognition of the moulding and its origin.

Dissolution de frustules à valves monolamellaires associée à un moulage phosphaté fruste. A: frustule non dissous; noter l'abondance des bâtonnets d'apatite entre les valves disjointes. La dissolution du frustule est très partielle en B, presque achevée en C et totale en D. En l'absence de fragment non dissous du test, la forme générale du moulage à structure très poreuse permet seule de reconnaître son origine.

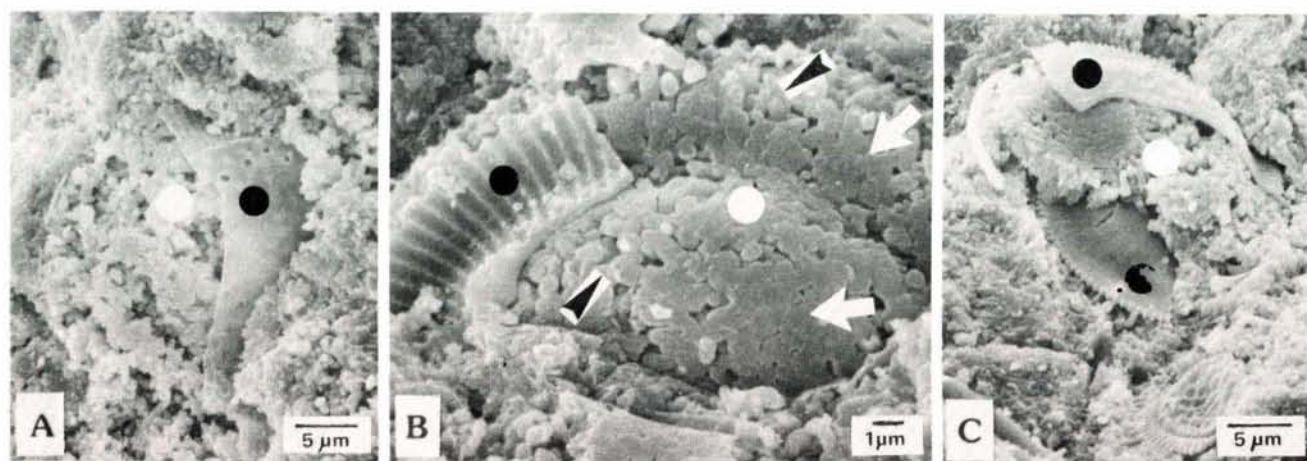


Figure 8

Accurate phosphatic moulding of frustules with monolamellar valves. Black dot=frustule. A part of the frustule was broken and removed during preparation of the sample, revealing its underlying phosphatic mould (white dot). In A, the phosphatic rod-shaped particles locally joined to the valve are flattened and coalesced. In B, flattening and coalescence is total in smooth regions (white arrows) but imperfect in rough regions (black arrows). In C, the phosphatic moulding, by complete coalescence of apatite particles, is locally almost as smooth as the internal surface of the lower valve.

Moulages phosphatés précis de frustules à valves monolamellaires. Rond noir=frustule. Une partie du frustule a été brisée et a disparu lors de la préparation du fragment, faisant apparaître son moulage phosphaté (rond blanc). En A, les bâtonnets d'apatite localement appliqués contre la valve sont aplatis et coalescents. En B, l'aplatissement et la coalescence sont totalement réalisés dans les zones lisses (flèches blanches) mais incomplets dans les zones rugueuses (flèches noires). En C, le moulage phosphaté (par coalescence complète des particules d'apatite) est localement presque aussi lisse que la surface interne de la valve inférieure.

(Fig. 7D) dissolution is often evident. Observations show that on the whole opal dissolution is quantitatively important both in the upper indurated part and in the lower pulverulent part. Frequently, opal dissolution appears to postdate phosphatization, but sometimes apatite fills a gap in the frustule, and opal dissolution must have occurred before apatite formation (Fig. 9C). Dissolution of diatom tests occurs in other phosphorites (Fig. 10) as does the dissolution of radiolarian tests (Azzouzi, 1989). In these cases, dissolution is generally complete. The first steps of opal dissolution observed in the Peruvian crust constitute a confirmation of the phenomenon and of its synchronism with phosphatization (Lamboy, 1987*b*).

In the topmost layer of the crust, the youngest part according to Kim and Burnett (1986), the present author has observed some fragments of planktonic foraminiferal tests and some carbonate particles undergoing dissolution. He has searched unsuccessfully in the rest of the crust for traces of coccoliths, foraminiferal tests and carbonate bioclasts and cannot assess the importance of carbonate dissolution. Dissolution of calcareous tests is frequently apparent in other phosphorites. In some cases, as in phosphatized fragments of echinoderm tests from Guinea Bissau, it has been shown that carbonate dissolution is synchronous with the formation of apatite particles (Lamboy, 1987*a*). The dissolution of opal and carbonate contributes to the enrichment of the sediment in solid phosphate, first by reducing the content of endogangue in phosphatic particles, second by creating new porosity susceptible to infilling by apatite. Such dissolution decreases information concerning the initial sediment.

Phosphatic mouldings of diatom tests

In the crust, some perfectly smooth small areas constituted by apatite correspond to the mouldings of non-

phosphatic hard particles. The great number and the various types of diatom tests, the possibility of distinguishing opaline tests from their phosphatic mouldings by means of SEM, and the frequent opal dissolution which permits observation of the morphology of the apatite previously connected to the test, make it possible to reconstitute this moulding process and to suggest an interpretation.

For diatoms whose valves have a monolamellar structure, the moulding is crude (Figs 7C, 7D) when only the general morphology of the test can be recognized. In this case, apatite particles constitute a very porous assemblage and those which are connected to the test are flattened. But the moulding is sometimes precise when the apatite particles are connected to the test, flattened and coalesced, locally (Fig. 8A) or against the whole valve (Fig. 8B). Their flattening and coalescence can finally produce a mould with a surface that is nearly as compact and smooth as the moulded surface (Fig. 8C). Similar mouldings of the external parts of the valves can also be observed.

For diatoms whose valves have a bilamellar structure, the internal and external moulds of the valves become more complicated because the moulding of the areoles, *i.e.* the intravalle cavities (Figs. 3A to 3D, 9A, 9B, 9D). Similar processes occur inside ferromanganese oceanic nodules (Janin, 1987). In the areoles, the rod-shaped apatite particles are irregularly distributed: they are either absent, isolated, grouped by two or more (Figs. 3A to 3D), or packed in glomerules which mould the areole cavity (fig. 9A). Opal dissolution allows us to observe flattening and coalescence of apatite particles against the test (Fig. 9B) resulting in a characteristic complex mould (Fig. 9D).

The inside of some diatom tests contain very few apatite particles, whereas others contain many. The phos-

phatic infilling of areoles is also irregular. This proves that, at the scale of microstructures, phosphatization is discontinuous and irregular in space. The flattening and coalescence of the apatite particles which constitute the moulding process are also irregularly distributed. However, although this is not self-evident, it seems that they are more numerous in the more indurated parts of the crust and may lead to more compact structures giving a greater hardness and a darker colour. Because flattening and coalescence occur here and there throughout the crust, they appear before overgrowth and/or recrystallization which are limited in the more evolved parts of this crust. The author believes that the moulding process may not be due to phosphatic crystal growth because, in this case, it has to take place inside the whole phosphatic matrix, rod-like particles

becoming coalescent within agglomerates, themselves becoming deformed one against the other.

The proposed bacterial interpretation perfectly explains the moulding process and the irregular repartition of phosphatic moulds, precise or not, inside the crust. Proliferation of bacteria varies from one area to another, probably according to the quantity or organic matter locally present. When bacteria abound, the bacterial bodies become flattened against the hard test and squashed together laterally. Phosphate mineralization removes the traces of this lateral squashing and leads to a more or less perfect coalescence. Quality of the moulding (*i.e.* compact and smooth surfaces) may be essentially due to the tight packing of bacterial bodies against the moulded surface and each other; the local denseness of bacteria proliferation. In the case of

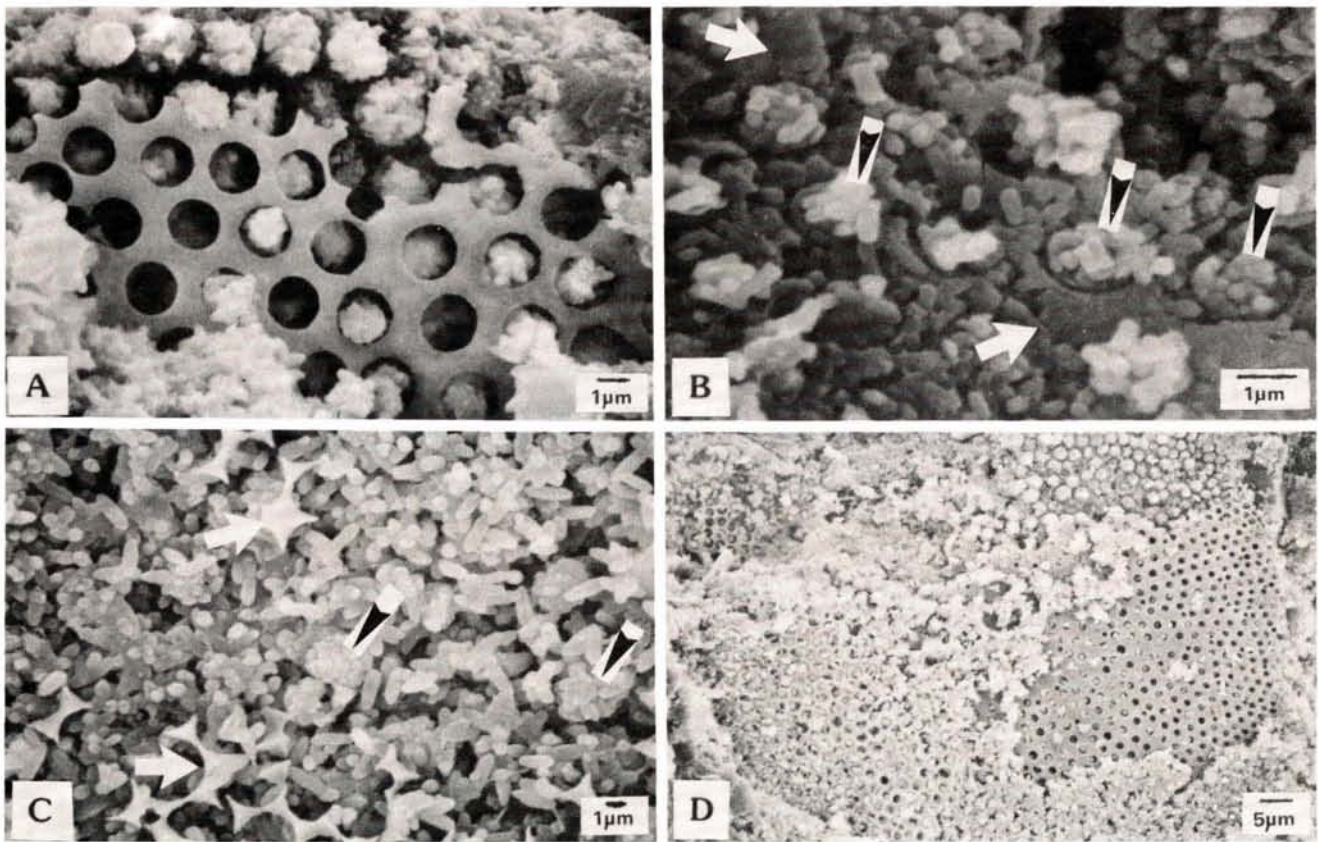


Figure 9

Phosphatic mouldings of frustule valves with a bilamellar structure. A: in the central part, rod-shaped apatite particles form glomerules inside the areoles (intravalve cavities located under large subcircular pores). They are not attached to the opal of the frustule. In the upper part, test dissolution reveals aligned glomerules which correspond to crude mouldings of areoles. B: the test is entirely dissolved. Between aligned areole mouldings (black arrows), some locally coalesced rod-shaped apatite particles build up an internal mould of the valve (white arrows). Here and there, some glomerules correspond to mouldings of areoles (black arrows). Between these elements and at the same level, rod-shaped apatite particles remain in place of the dissolved test. They thus formed after test dissolution, without nucleation on opal. D: from place to place, the walls of the valves may or may not be present, but the structure of the diatom test can always be recognized with either a precise or a rough phosphatic moulding. There is no proof of apatite nucleation on the frustule. Some of these phenomena can also be seen on figure 3 (A, B, C). The interpretation of rod-shaped particles as phosphatized bacteria perfectly explains: (i) the variable infilling of cavities, corresponding to the non-systematic, somewhat intense bacterial colonization; and (ii) the variable precision of the moulding, due to more or less flattened and coalesced bacterial bodies.

Moulanges phosphatés de frustules à valves de structure bilamellaire. A: dans la partie centrale, les bâtonnets forment des glomérules occupant les aréoles (cavités intravalvaires situées sous les gros pores subcirculaires). Ils ne sont pas fixés à l'opale du frustule. Dans la partie supérieure, la dissolution du test permet de voir des glomérules alignés, moulages grossiers d'aréoles. B: le test est totalement dissous; entre les moules d'aréoles alignés (flèches noires), des bâtonnets localement coalescents constituent un moulage interne de la valve (flèches blanches). C: les restes de couleur claire d'une paroi de frustule non dissoute sont visibles (flèches blanches); ça et là, quelques glomérules correspondent au moulage d'aréoles (flèches noires). Entre ces éléments et au même niveau, des bâtonnets d'apatite sont à l'emplacement du test dissous; ils se sont formés nécessairement après la dissolution du test, sans nucléation sur de l'opale. D: d'un endroit à l'autre, les parois des valves du frustule sont présentes ou dissoutes, avec soit un moulage phosphaté précis soit un moulage peu conservatif des structures. On ne peut prouver la nucléation de l'apatite sur le frustule. Certains de ces phénomènes sont également visibles sur la figure 3 (A, B, C). L'interprétation des bâtonnets d'apatite comme des bactéries phosphatisées explique parfaitement: 1) le remplissage variable des cavités, correspondant à une colonisation bactérienne non systématique et parfois intense, 2) la précision variable du moulage, due à l'aplatissement et à la coalescence plus ou moins prononcés des corps bactériens.

phatic infilling of areoles is also irregular. This proves that, at the scale of microstructures, phosphatization is discontinuous and irregular in space. The flattening and coalescence of the apatite particles which constitute the moulding process are also irregularly distributed. However, although this is not self-evident, it seems that they are more numerous in the more indurated parts of the crust and may lead to more compact structures giving a greater hardness and a darker colour. Because flattening and coalescence occur here and there throughout the crust, they appear before overgrowth and/or recrystallization which are limited in the more evolved parts of this crust. The author believes that the moulding process may not be due to phosphatic crystal growth because, in this case, it has to take place inside the whole phosphatic matrix, rod-like particles

becoming coalescent within agglomerates, themselves becoming deformed one against the other. The proposed bacterial interpretation perfectly explains the moulding process and the irregular repartition of phosphatic moulds, precise or not, inside the crust. Proliferation of bacteria varies from one area to another, probably according to the quantity or organic matter locally present. When bacteria abound, the bacterial bodies become flattened against the hard test and squashed together laterally. Phosphate mineralization removes the traces of this lateral squashing and leads to a more or less perfect coalescence. Quality of the moulding (*i.e.* compact and smooth surfaces) may be essentially due to the tight packing of bacterial bodies against the moulded surface and each other; the local denseness of bacteria proliferation. In the case of

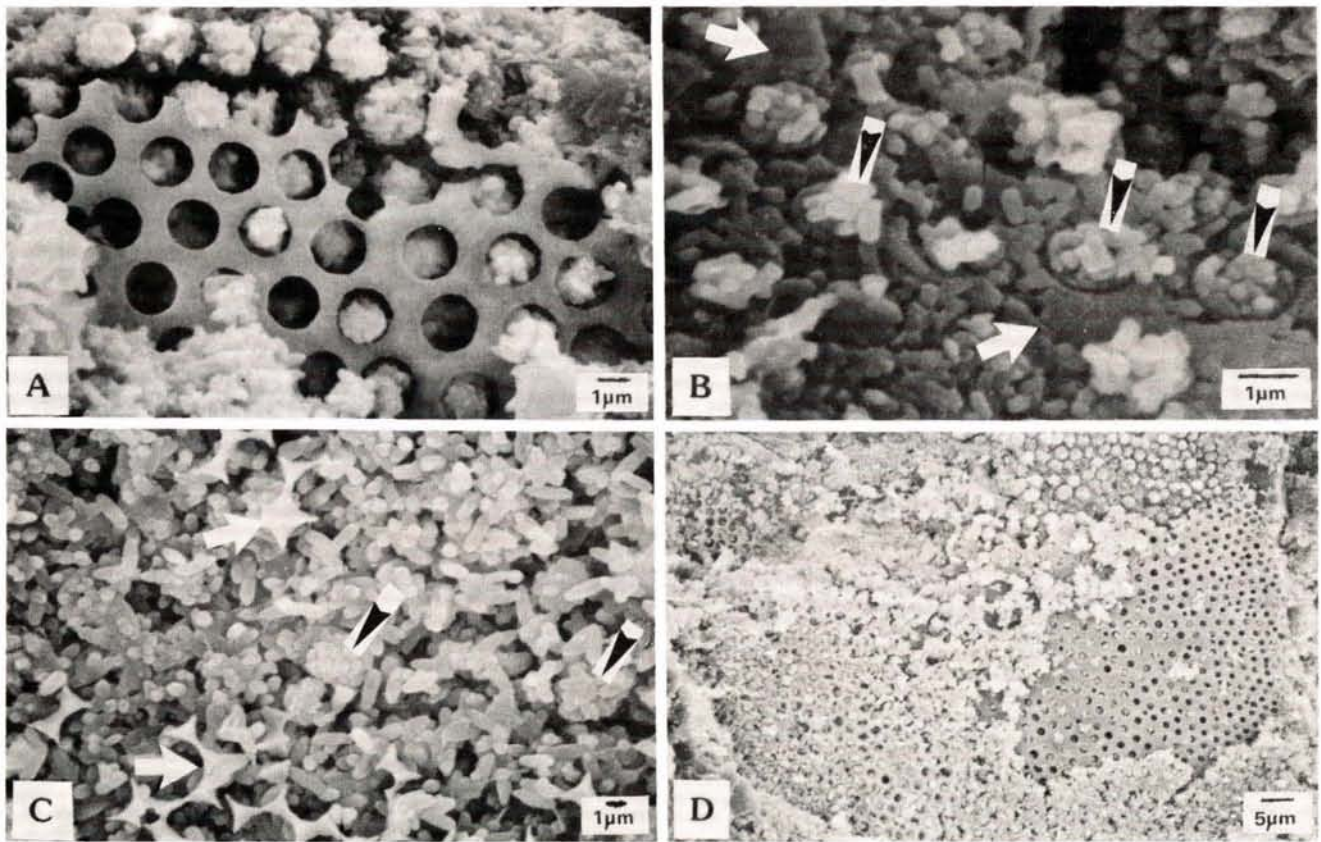


Figure 9

Phosphatic mouldings of frustule valves with a bilamellar structure. A: in the central part, rod-shaped apatite particles form glomerules inside the areoles (intravalve cavities located under large subcircular pores). They are not attached to the opal of the frustule. In the upper part, test dissolution reveals aligned glomerules which correspond to crude mouldings of areoles. B: the test is entirely dissolved. Between aligned areole mouldings (black arrows), some locally coalesced rod-shaped apatite particles build up an internal mould of the valve (white arrows). C: some light-coloured, non-dissolved remains of a frustule valve are visible (white arrows). Here and there, some glomerules correspond to mouldings of areoles (black arrows). Between these elements and at the same level, rod-shaped apatite particles remain in place of the dissolved test. They thus formed after test dissolution, without nucleation on opal. D: from place to place, the walls of the valves may or may not be present, but the structure of the diatom test can always be recognized with either a precise or a rough phosphatic moulding. There is no proof of apatite nucleation on the frustule. Some of these phenomena can also be seen on figure 3 (A, B, C). The interpretation of rod-shaped particles as phosphatized bacteria perfectly explains: (i) the variable infilling of cavities, corresponding to the non-systematic, somewhat intense bacterial colonization; and (ii) the variable precision of the moulding, due to more or less flattened and coalesced bacterial bodies.

Moulages phosphatés de frustules à valves de structure bilamellaire. A: dans la partie centrale, les bâtonnets forment des glomérules occupant les aréoles (cavités intravalvaires situées sous les gros pores subcirculaires). Ils ne sont pas fixés à l'opale du frustule. Dans la partie supérieure, la dissolution du test permet de voir des glomérules alignés, moulages grossiers d'aréoles. B: le test est totalement dissous; entre les moules d'aréoles alignés (flèches noires), des bâtonnets localement coalescents constituent un moulage interne de la valve (flèches blanches). C: les restes de couleur claire d'une paroi de frustule non dissoute sont visibles (flèches blanches); ça et là, quelques glomérules correspondent au moulage d'aréoles (flèches noires). Entre ces éléments et au même niveau, des bâtonnets d'apatite sont à l'emplacement du test dissous; ils se sont formés nécessairement après la dissolution du test, sans nucléation sur de l'opale. D: d'un endroit à l'autre, les parois des valves du frustule sont présentes ou dissoutes, avec soit un moulage phosphaté précis soit un moulage peu conservatif des structures. On ne peut prouver la nucléation de l'apatite sur le frustule. Certains de ces phénomènes sont également visibles sur la figure 3 (A, B, C). L'interprétation des bâtonnets d'apatite comme des bactéries phosphatisées explique parfaitement: 1) le remplissage variable des cavités, correspondant à une colonisation bactérienne non systématique et parfois intense, 2) la précision variable du moulage, due à l'aplatissement et à la coalescence plus ou moins prononcés des corps bactériens.

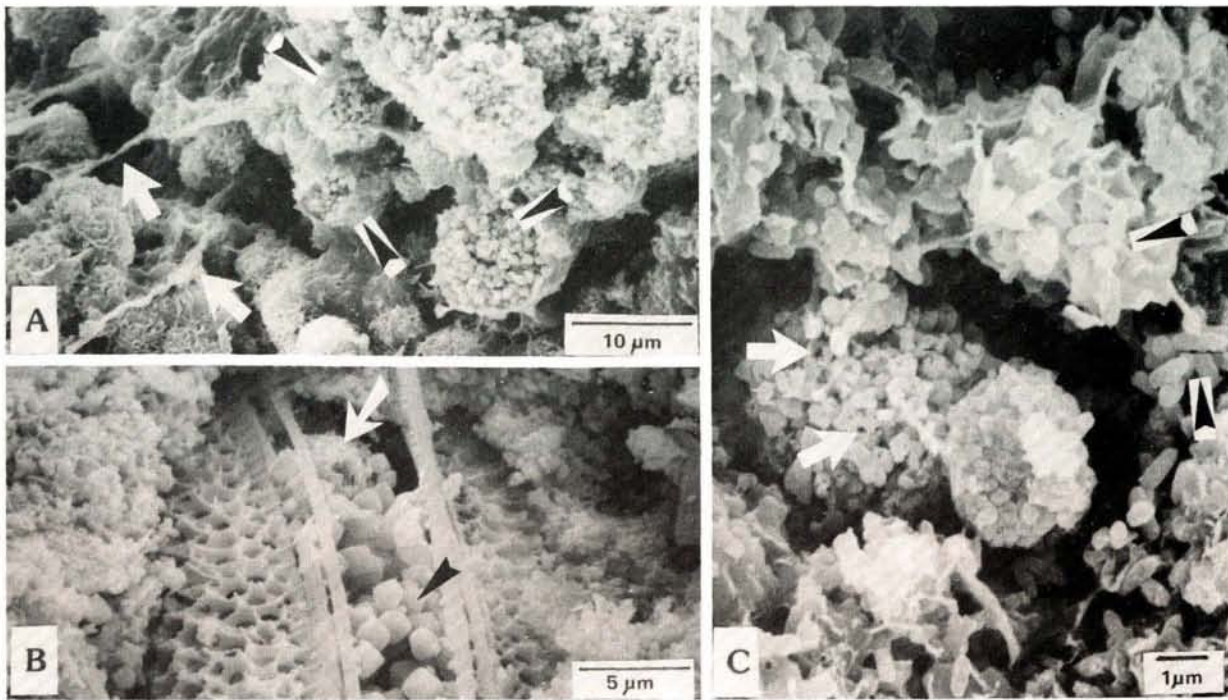


Figure 11

Some aspects of pyrite associated with apatite. A: wall of a crack in a glauconite grain; the pyrite framboids (black arrows) coated with organics (?) are associated with organic filaments (white arrows) that cross the surface of the glauconite plates. B: agglomerated rod-like apatite particles surround a frustule which contains a framboid (white arrow) and microcrystals of pyrite (black arrow). C: periphery of a glauconite grain; in the centre, two pyrite framboids are in a cavity (note the hollow crystals, white arrows); around it, rod-shaped apatite particles (black arrows) are associated with contorted glauconite plates.

Aspects de la pyrite associée à l'apatite. A: intérieur d'une fissure d'un grain de glauconite; les framboïdes de pyrite (flèches noires), entourés de leur enveloppe organique (?), sont associés à des filaments organiques (flèches blanches) qui courent à la surface des lamelles de glauconite. B: les bâtonnets d'apatite entourent un frustule renfermant un framboïde (flèche blanche) et des microcristaux de pyrite (flèche noire). C: périphérie d'un grain de glauconite; au centre, deux framboïdes de pyrite sont dans une cavité (noter les cristaux creux, flèches blanches); latéralement, des bâtonnets d'apatite (flèches noires) sont associés aux lamelles flexueuses de glauconite.

Therefore, there is evidence that the process of moulding (microbially mediated or not), often prominently revealed by dissolution, is a characteristic phenomenon in numerous phosphorites (Lambooy, 1987*b*) and a factor in the genesis of these phosphorites.

Glauconite and pyrite associated with apatite

Glauconite appears as light green and dark green grains irregularly scattered throughout the crust (Fig. 1). Glauconite grains are rounded and cracked in their outer parts. The recognition of the initial granular support (Odin, 1988) is not possible. Broken parts often show packed contorted blades. All of these observations point to the evolved nature of glauconite which is confirmed by a rather high content in potassium (5.8% K²⁰ on average) (Odin, 1988). Rod-shaped apatite particles are present in cracks of glauconite grains and occur between the glauconitic blades at the periphery of glauconite grains (Fig. 11 C). Thus, these observations confirm that glauconite grains are earlier than phosphate (Glenn and Arthur, 1988), and it seems that bacteria must have penetrated into microcavities of glauconite grains, as they did in those of other substrates.

Small dots of pyrite are scattered throughout the crust, particularly in its lower part and in small cavities. Coupled SEM and microprobe permit the observation of framboids and microcrystals of pyrite which are

intimately mixed with apatite. The framboids, 5 to 10 μm in diameter, composed of numerous small, globular crystals, often hollow (Fig. 11 C), are clearly visible in cracks of glauconite grains (Fig. 11 A). The presence of filaments and apparently organic envelopes around framboids points to the role of bacterial activity in pyrite precipitation (Monty, 1981). Often octahedral pyrite microcrystallites, 1 to 5 μm in size, are associated with framboids (Fig. 11 B). Because of the small size of pyrite and apatite crystals, and because of the complexity of the structures, it is very difficult to deduce structural arguments which could explain the intimate juxtaposition of pyrite and apatite crystals. The diagenetic and paragenetic sequence proposed by Glenn and Arthur (1988) for Peru margin organic-rich sediments is not complete in the crust studied here, which does not contain dolomite. For these authors, precipitation of apatite and pyrite appears to be nearly coincidental, with pyrite precipitation continuing after that of apatite. Indeed, it appears that framboids are preferentially localized in cavities which were still empty after the end of phosphatization (Fig. 11 C). In the hypothesis of a microbial origin for pyrite framboids, synchronism and diachronism with apatite formation could be explained by the necessity of anoxic microenvironments for microbes producing the H²S required for pyrite formation (Altschuler *et al.*, 1983; Berner, 1985). This anoxia could be progressively established by decomposition of organic matter during sediment burial (Berner, 1985; Ingall and Van Cappellen, 1989).

CONCLUSION

Crust GS 1N contains some glauconite grains, diatom frustules, and small detrital particules scattered in an abundant, homogeneous, fine-grained apatite matrix corresponding to the interstitial phosphatic cements described by Glenn and Arthur (1988). This SEM study shows that, in this crust, phosphatization occurs without modification of the initial sediment volume, and with the preservation of at least part of the sediment structures. At the scale of microstructures, phosphatization is discontinuous and irregular in space and time. The apatite particles form in inter- and intra-granular pore spaces, probably filled with organic matter, apparent without nucleation on the walls of the pore spaces.

Opal dissolution of diatom frustules occurs here and there inside the crust, creating new porosity which is sometimes utilized for apatite growth. It decreases the "memory" of the initial sediment composing the crust. These phenomena, which can be observed in other phosphorites, are comparable to those associated with the dissolution of carbonate tests which have been described in other phosphorites (Lamboy, 1989).

The replacement of diatom opal by apatite has not been observed in the crust. The conservation of frustule structures observed in thin section corresponds to more or less precise mouldings by apatite. In a sense, apatite moulding partially compensates for the loss of information due to opal dissolution. The structural data

gathered in the present study are coherent with those of studies of other phosphorites using the same methods (Lamboy, 1987b, 1988, 1989; Fikri *et al.*, 1989) and concerning apatite mouldings of carbonate tests.

The rod-shaped apatite particles constituting the bulk of the crust are sometimes intimately mixed with framboids and microcrystals of pyrite. The detailed analysis of these apatite particles and of the associated structures brings new qualitative and quantitative arguments in favour of bacterial phosphatization. Bacteria invade a specific portion of the sediment and are later mineralized into apatite. Overgrowth around a bacterial body and/or recrystallization ultimately leads to an elongated hexagonal microprism of apatite.

Acknowledgements

I am deeply indebted to W. C. Burnett who kindly furnished the crust fragment and accepted numerous discussions. I am pleased to thank G. Ehret (University of Strasbourg) for preparing samples for TEM observations, and taking the photomicrograph of figure 5B. For discussions, generous access to unpublished data, and improvement of the English text of the manuscript, I am very grateful to Z. S. Altschuler, P. Van Cappellen and K. Föllmi. I also wish to thank C. R. Glenn for his critical reviews of the manuscript and for his very constructive comments.

REFERENCES

- Altschuler Z. S., M. M. Schnepfe, C. C. Silber, F. O. Simon (1983). Sulfur diagenesis in Everglades peat and origin of pyrite in coal. *Science*, **221**, 221-227.
- Azzouzi N. (1989). Contribution à l'étude des phosphates marocains: approche de la phosphatogenèse dans le gisement des Ouled-Abdoun. *Colloque de Géologie franco-marocain*, Strasbourg, résumés, 20.
- Baker K. B., W. C. Burnett (1988). Distribution, texture and composition of modern phosphate pellets in Peru shelf muds. *Mar. Geol.*, **80**, 195-213.
- Baturin G. N. (1982). Phosphorites on the sea floor. Origin, composition and distribution. *Developments in sedimentology*, **33**, 343 p.
- Baturin G. N., V. T. Dubinchuk (1979). Microstructures of marine phosphorites: atlas of microphotographs. *Izdat. Nauka*, Moscow, 198 p. (in Russian). French translation n° 959, (1981) BRGM, Orléans.
- Bayer G., H. G. Wiedemann (1989). Kinetics of formation of Ca WO₄ and MoO₄ from calcium carbonates and sulfates. *American Lab.*, **21**, 1, 40-47.
- Ben Amar Z. (1985). Contribution à l'étude des phosphates de Jellabia (bassin de Gafsa, Tunisie). *Thesis*, Université de Rouen, 185 pp.
- Berner R. A. (1985). Sulphate reduction, organic matter decomposition and pyrite formation. *Phil. Trans. R. Soc. Lond.*, **315**, 25-38.
- Bréhéret J. G. (1990). Phosphatic concretions in black facies of the mid-Cretaceous marls of the Vocontian Basin (SE France) and in site 369 D.S.D.P.: witnesses of benthic microbial activity. *Mar. Geol. sp. publ.*, to be published.
- Bremner J. M. (1980). Concretionary phosphorite from SW Africa. *J. Geol. Soc. London*, **137**, 773-786.
- Burnett W. C. (1977). Geochemistry and origin of phosphorite deposits from off Peru and Chile. *Geol. Soc. Amer. Bull.*, **88**, 813-823.
- Burnett W. C., H. H. Veeh, A. Soutar (1980). U-Series, oceanographic and sedimentary evidence in support of recent formation of phosphate nodules off Peru. *Marine Phosphorites a symposium, SEPM sp. publ. n° 29*, 61-71.
- Burnett W. C., K. H. Kim (1986). Comparison of radiocarbon and uranium series dating methods as applied to marine apatite. *Quat. Res.*, **25**, 369-379.
- Burnett W. C., P. N. Froelich (1988). The origin of marine phosphorite. The results of the RV Robert D. Conrad cruise 23-06 to the Peru shelf; preface. *Mar. Geol.*, **80**, III-VI.
- Chaabani F. (1978). Les phosphorites de la coupe-type de Fom Selja (Metlaoui, Tunisie). Une série sédimentaire séquentielle à évaporites du Paléogène. *Thesis*, University of Strasbourg, 131 p.
- Costerton J. W., G. G. Geesey, K. J. Cheng (1978). Comment collent les bactéries. *Pour la Science*, **5**, 100-110.
- Cullen D. J., W. C. Burnett (1986). Phosphorite associations on seamounts in the tropical southwest Pacific Ocean. *Mar. Geol.*, **71**, 215-236.
- Cunningham R., W. C. Burnett (1985). Amino-acid biogeochemistry and dating of offshore Peru-Chile phosphorites. *Geochim. Cosmochim. Acta*, **49**, 1413-1419.
- El Faleh E. (1988). Les mécanismes de synthèse de l'apatite par activité bactérienne; rôle et comportement de quelques éléments minéraux. Application aux phosphates sédimentaires. *Thesis*, University of Strasbourg, 230 p.
- Fikri A., M. Lamboy, S. Benalioulaj, J. Trichet, H. Belayouni (1989). Contribution à l'étude pétrologique de la matière organique dans les phosphates naturels. Nouvelles approches méthodologiques. *Bull. Soc. Géol. France*, **8**, 5, 979-987.
- Froelich P. N., M. Arthur, W. C. Burnett, M. Deakin, V. Hensley, R. Jahnke, L. Kaul, K. H. Kim, K. Roe, A. Souta, C. Vathakanon

- (1988). Early diagenesis of organic matter in Peru continental margin sediments: Phosphorite precipitation. *Mar. Geol.*, **80**, 309-343.
- Garrison R. E., M. Kastner, Y. Kolodny (1987). Phosphorites and phosphatic rocks in the Monterey Formation and related miocene units, coastal California. In Gersol R. V. and Ernst W. G. (ed.), Rubey vol.: Englewood cliffs N. J. Cenozoic Basin development in coastal California, **6**, 348-381.
- Glenn C. R., M. A. Arthur (1988). Petrology and major element geochemistry of Peru margin phosphorites and associated diagenetic minerals: Authigenesis in modern organic-rich sediments. *Mar. Geol.*, **80**, 231-267.
- Glenn C. R., M. A. Arthur, H. W. Yeh, W. C. Burnett (1988). Carbon isotopic composition and lattice-bound carbonate of Peru-Chile margin phosphorites. *Mar. Geol.*, **80**, 287-307.
- Ingall E. D., P. Van Cappellen (1990). Relation between sedimentation rate and burial of organic phosphorus and organic carbon in marine sediments. *Geochim. Cosmochim. Acta*, **54**, 373-386.
- Jahnke R. A., S. R. Emerson, K. K. Roc, W. C. Burnett (1983). The present-day formation of apatite in Mexican continental margin sediments. *Geochim. Cosmochim. Acta*, **47**, 259-266.
- Janin M. C. (1987). Micropaléontologie de concrétions polymétalliques du Pacifique central. *Mém. Soc. Géol. France*, Paris, **152**, 317 p.
- Janin M. C. (1987). Micropaleontology of manganese nodules from the equatorial North Pacific Ocean. Area SO 25-1 and SO 25-3. *Geol. Jb.*, D87, 315-375.
- Kim K. H., W. C. Burnett, (1985). ^{226}Ra in marine phosphate nodules from Peru Chile seafloor. *Geochim. Cosmochim. Acta*, **49**, pp. 1073-1081.
- Kim K. H., W. C. Burnett (1986). Uranium-series growth history of a Quaternary phosphatic crust from the Peruvian continental margin. *Chemical Geology (Isotope Geoscience Section)*, **58**, 227-244.
- Kim K. H., W. C. Burnett (1988). Accumulation and biological mixing of Peru margin sediments. *Mar. Geol.*, **80**, 181-194.
- Kolodny Y. (1982). Phosphorites. In: *The oceanic lithosphere*, Emiliani ed., The sea, **7**, 981-1023.
- Lambo M. (1987a). Genèse de grains de phosphate à partir de débris de squelette d'échinodermes: les processus et leur signification. *Bull. Soc. géol. France*, **8**, 3, 759-768.
- Lambo M. (1987b). The role of microbes in the genesis of phosphatic grains. I.G.C.P., project 156: phosphorites, International field workshop and symposium, Tunis, Abstracts.
- Lambo M. (1988). New data related to the petrography and the genesis of granular phosphorites. I.G.C.P., project 156: phosphorites, Regional meeting on cretaceous and tertiary phosphorites, Amman, Abstracts, p. 15.
- Lambo M. (1990). Microbial mediation in phosphatogenesis: new data from the Cretaceous phosphatic chalks of northern France. I.G.C.P., project 156: phosphorites, 11th international field workshop and symposium: a decade of phosphorite research and development, Oxford, Abstracts p. 15; and in: A. Notholt and I. Jarvis eds, Phosphorite Research and Development, *Geol. Soc. of London*, sp. publ., **52**, 157-167.
- Lambo M., C. Monty (1987). Bacterial origin of phosphatized grains. *Terra Cognita*, **7**, p. 207.
- Lambo M., C. Monty (1990). Observations on microbial precipitation of phosphate. *Mar. Geol. sp. publ.*, to be published.
- Lucas J., L. Prévôt (1981). Synthèse d'apatite à partir de matière organique phosphorée (ARN) et de calcite par voie bactérienne. *C.R. Acad. Sci.*, **292**, 1203-1208.
- Lucas J., L. Prévôt (1985). The synthesis of apatite by bacterial activity: mechanism. *Sci. Geol. Mém.*, **77**, 83-92.
- Lucas J., L. Prévôt (1988). The mechanisms of biochemical synthesis of apatite: statement of teamwork in Strasbourg. I.G.C.P., project 156: phosphorites, 11th international field workshop and symposium: a decade of phosphorite research and development, Oxford Abstracts.
- Monty C. L. (1981). Observations pétrographiques et chimiques sur l'éodiagenèse de carbonates du précontinent calvais (Corse). *Bull. Soc. royale des Sc. de Liège*, **11-12**, 470-482.
- Mullins H. T., R. F. Rasch (1985). Sea-floor phosphorites along the Central California continental margin. *Economic Geology*, **80**, 696-715.
- O'Brien G. W., H. H. Veeh (1980). Holocene phosphorite on the East Australian continental margin. *Nature*, **288**, 690-692.
- O'Brien G. W., J. R. Harris, A. R. Milnes, H. H. Veeh (1981). Bacterial origin of East Australian continental margin phosphorites. *Nature*, **294**, 442-444.
- Odin G. S. (1988). Green marine clays. *Developments on sedimentology*, **45**, 445 p.
- Piper D. Z., P. A. Baedecker, J. G. Crock, W. C. Burnett, B. J. Loebner (1988). Rare earth elements in the phosphatic-enriched sediments of the Peru shelf. *Mar. Geol.*, **80**, 269-285.
- Prévôt L., J. Lucas (1986). Microstructure of apatite-replacing carbonate in synthesized and natural samples. *Journ. of Sedim. petrology*, **56**, 153-159.
- Purnachandra Rao V., R. R. Nair (1988). Microbial origin of the phosphorites of the western continental shelf of India. *Mar. Geol.*, **84**, 105-110.
- Purnachandra Rao V., W. C. Burnett. Phosphatic rocks from seam-vents in the eoz of Kiribati and Tuvalu, central Pacific ocean Geology and offshore Mineral resources of the central Pacific basin, B. Keating and B. Bolton eds., AAPG-circum Pacific monographs series, in press.
- Reimers C. E. (1982). Organic matter in anoxic sediments off central Peru: relations of porosity, microbial decomposition and deformation properties. *Mar. Geol.*, **46**, 175-197.
- Reimers C. E., M. Kastner, R. E. Garrison (1990). The role of bacterial mats in phosphate mineralization with particular reference to the Monterey Formation. In: Genesis of Neogene to Modern Phosphorites, W. C. Burnett and S. R. Riggs eds. Cambridge Univ. Press, in press.
- Slansky M. (1980). Géologie des phosphates sédimentaires. *Mém. B.R.G.M.*, Orléans, **114**, 92 p.
- Slansky M. (1986). Geology of sedimentary phosphates. In: Studies in Geology, North Oxford Academic ed., Oxford and B.R.G.M., Orléans, 210 p.
- Soudry D. (1987). Ultra-fine structures and genesis of the Campanian Negev high-grade phosphorites (southern Israel). *Sedimentology*, **34**, 641-660.
- Soudry D., Y. Champetier (1983). Microbial processes in the Negev phosphorites (southern Israel). *Sedimentology*, **30**, 411-423.
- Soudry D., Z. Lewy (1988). Microbially influenced formation of phosphate nodules and megafossil moulds (Negev, southern Israel). *Palaeogeogr. Palaeoclim. Palaeoec.*, **64**, 15-34.
- Soudry D., P. N. Southgate (1989). Ultrastructure of a middle Cambrian nonpelletal phosphorite and its early transformation. into phosphate vadoids: Georgina basin, Australia. *Journ. of Sedim. Petrology*, **59**, 53-64.
- Southgate P. N. (1986). Cambrian phosphorete profiles, coated grains, and microbial processes in phosphogenesis: Georgina Basin, Australia. *Journ. of Sedim. Petrology*, **56**, 429-441.
- Vaillant B. (1987). Étude expérimentale du rôle de flores bactériennes dans la formation de l'apatite. *Thesis*, University of Nancy, 167 p.
- Van Cappellen P., R. A. Berner (1988). A mathematical model for the early diagenesis of phosphorus and fluorine in marine sediments: apatite precipitation. *Amer. Journ. of Sci.*, **228**.
- Van Cappellen P., R. A. Berner (1989). Marine apatite formation. In: Water-Rock Interaction, (WRI-6), D. L. Miles ed., A. A. Balkema Rotterdam. 707-710.
- Veeh H. H., W. C. Burnett, A. Soutar (1973). Contemporary phosphorites on the continental margin of Peru. *Science*, **181**, 844-845.
- Williams L. A., C. Reimers (1983). Role of bacterial mats in oxygen deficient marine basins and coastal upwelling regimes: Preliminary Report. *Geology*, **11**, 267-269.
- Zanin Y. N., S. V. Letov, N. A. Krasil'nikova, Y. V. Mirtov (1985). Phosphatized bacteria from Cretaceous phosphorites of European platform and Paleocene phosphorites of Morocco. *Sci. Geol. Mém.*, **77**, 79-81.
- Zanin Y., V. Gorlenko, Y. Mirtov, N. A. Krasil'nikova, S. Letov (1987). Bacteriomorphic formations in nodular and granular phosphorites. *Soviet Geology and Geophysics*, **28**, 2, 39-44.